Time-dependent properties of classical artificial atoms

1998 J. Phys.: Condens. Matter 10 2417

(http://iopscience.iop.org/0953-8984/10/11/006)

J. Phys.: Condens. Matter **10** (1998) 2417–2435. Printed in the UK PII: S0953-8984(98)85240-5

Time-dependent properties of classical artificial atoms

V A Schweigert† and F M Peeters‡

Departement Natuurkunde, Universiteit Antwerpen (UIA), Universiteitsplein 1, B-2610 Antwerpen, Belgium

Received 20 June 1997

Abstract. The time-dependent properties of a finite number of classical charged particles moving in two dimensions (2D) and which are confined by a parabolic potential are studied. In equilibrium those particles arrange themselves in shells. Using molecular dynamics we obtain the temperature dependence of the transition rate for particles jumping between shells and the transition rate for intershell rotation. The temperature dependence of the velocity autocorrelation function is studied. We relate the behaviour of these quantities to the melting of the system. The results of our numerical simulation are compared with those from classical rate theory. The influence of a magnetic field on the particle motion and on the rate of jumps is also investigated.

1. Introduction

Currently, a lot of theoretical and experimental investigations are devoted to mesoscopic systems consisting of a finite number of particles. A cluster of charged particles, called an 'artificial atom' confined by an external potential is an example of such a system. Although most of such systems are inherently quantum mechanical they often exhibit many classical mechanical features. Here we will limit ourselves to pure classical considerations neglecting any quantum nature of the particles. For two-dimensional (2D) clusters of charged particles which are confined by a parabolic potential, the ordered structures consist of particles which are arranged in shells. A Mendeleev type of table was constructed in reference [1] for these 'classical atoms'. The melting temperature and the excitation spectrum of the normal modes were obtained in references [2, 3]. The purpose of the present paper is to study the time evolution of this system, or equivalently the Fourier transform of it, and to correlate it with the ordered and liquid states of this finite system.

The melting of the ordered 2D cluster was considered by Lozovik and co-authors in references [4, 5] using the method of molecular dynamics. These authors have found that a cluster consisting of not too many particles ($N < 50$) does not have a well defined melting temperature, and that the transition for intershell diffusion occurs at a higher temperature than the one for intershell rotational diffusion. Bedanov and Peeters [1] have used Monte Carlo simulations to obtain the temperature dependence of the variation in the mean radial and axial displacements of particles from their equilibrium position and the square intershell deviations. Analysing the computed mean square displacement with the Lindemann criterion these authors were able to define two different melting temperatures.

† Permanent address: Institute of Theoretical and Applied Mechanics, Russian Academy of Sciences, Novosibirsk 630090, Russia.

‡ E-mail: peeters@uia.ua.ac.be.

0953-8984/98/112417+19$19.50

There are a number of problems associated with the calculation of the melting temperature in the case of finite systems:

(1) rates of intershell rotation and intershell jumps have finite values for any temperature, even though they decrease exponentially with decreasing temperature;

(2) for a cluster of N particles the mean square displacement $\Delta = N^{-1}\sum_{i=1}^{N}(\langle \boldsymbol{r}_i{}^2\rangle - \langle \boldsymbol{r}_i\rangle^2)$ reaches a finite non-zero value after some time which is set by the scale of the vibration frequency of the cluster.

Then as a result of intershell rotation or of transitions of the particles between shells, the mean square displacement first starts to grow linearly with time and then for large times achieves a final value which is determined by the size of the system. Although the particle motion which we have observed is diffusive in nature, it is obvious that the self-diffusion coefficient $D = \lim_{t\to\infty}\Delta(t)/t$ is zero for any finite system. Therefore the standard approach for calculating the diffusion coefficient and the mean square displacement is only applicable for a finite time interval [6]. Indeed, for $t \to \infty$ the diffusion coefficient tends to zero while the latter grows as function of time and exceeds the mean interparticle distance. Because, for axial symmetric external potentials, the frequencies of the different normal modes can change by orders of magnitude as was found in reference [2], there are additional difficulties in defining a time interval in which the self-diffusion coefficient and the mean square displacement can be reliably defined.

Because of the above difficulties, we present in this paper an alternative method for obtaining information on melting by using rates of intershell rotation and intershell jumps as the characteristics of the non-zero-temperature particle motion in such finite systems. We have obtained the temperature dependence of the rate of intershell rotation and intershell jumps for clusters with different numbers of particles. We also evaluated the influence of a magnetic field on the particle motion and explored the behaviour of the velocity autocorrelation function for different temperatures.

The paper is organized as follows. In section 2, we state the problem and describe our simulation method. Section 3 is devoted to the results of our simulation for the rate of intershell rotation. In section 4, the mechanism for the intershell jump rate is investigated. In section 5, we consider the behaviour of the velocity autocorrelation function. The influence of a magnetic field on the particle motion is investigated in section 6. The conclusions of the present work are given in section 7.

2. The model system and numerical approach

To study the time dependence of a system consisting of 2D charged particles which are confined by a parabolic potential we use the numerical simulation technique of molecular dynamics. Using dimensionless units, we can write the system of Newton equations which govern the time evolution of the particles in our cluster in the presence of a magnetic field $\boldsymbol{B}$ (taken along the z-axis) as

$$\frac{\partial^2 \boldsymbol{r}_i}{\partial t^2} = -\frac{\partial U(\boldsymbol{r}_i)}{\partial \boldsymbol{r}_i} + \frac{\partial \boldsymbol{r}_i}{\partial t} \times \boldsymbol{\omega}_c \tag{1}$$

where

$$U = \sum_{i>j=1}^{N} \frac{1}{|\boldsymbol{r}_i - \boldsymbol{r}_j|} + \sum_{i=1}^{N} \boldsymbol{r}_i{}^2 \tag{2}$$

is the total potential energy. Here the time is measured in units of $\sqrt{2}/\omega_0$, the frequency in units of $\omega_0/\sqrt{2}$, the distance in units of $(2q^2/m\epsilon\omega_0^2)^{-1/3}$, and the energy and temperature in units of $(m\omega_0^2q^4/2\epsilon^2)^{1/3}$, where ω_0 is the vibration frequency of a single particle in the parabolic confinement potential, m is the mass of the particle, $\boldsymbol{\omega}_c = (0, 0, \omega_c)$ where $\omega_c = qB/mc$ is the cyclotron frequency, q is the particle charge, and ϵ is the static dielectric constant of the medium that the particles are moving in.

In a strong magnetic field the cyclotron frequency exceeds the typical vibration frequency of a particle near its equilibrium position. In this case, common schemes solving the Newton equations (for example, see reference [7]) can no longer be used, because in such a case the time step will be determined by the cyclotron frequency. Therefore, in the present paper the construction of a finite-difference scheme is based on the use of the explicit solutions of the Newton equations for a constant force (see e.g. reference [8]) in a uniform magnetic field. Because we consider uniform magnetic fields the accuracy of the algorithm will therefore be independent of the cyclotron frequency. The force which acts on the particle is defined by the predictor–corrector method. The time step is determined from the condition that the total energy may not change by more than 0.1% during the simulation.

We consider mainly the motion of the particles at non-zero temperature. The initial conditions for the system of equations (1) were found in the following way. An initial particle configuration was chosen as the ground state (see reference [2]). Then we executed 10^4–10^5 steps of the standard Metropolis algorithm [9] at some temperature T to allow the system to approach its equilibrium state. Then we determined the initial values for the velocity of the particles $\boldsymbol{v}_i'$ by using the Maxwellian probability distribution $f(\boldsymbol{v}_i') = (1/2\pi T)\exp(-v_i'^2/2T)$ in combination with a random-number generator. Furthermore we used the transformation

$$\boldsymbol{v}_i = \boldsymbol{v}_i' + \boldsymbol{r}_i \times \sum_i [\boldsymbol{r}_i \times \boldsymbol{v}_i'] \Big/ \sum_i \boldsymbol{r}_i{}^2$$

in order to exclude uniform rotations of the cluster as a whole. Consequently, the particle motion is calculated for fixed energy using the method of molecular dynamics. This gives us the time evolution of the particle coordinates and its velocities. For the averages over the energy, about 40–60 initial configurations were generated in phase space. The statistical error resulting from the use of a finite number of initial configurations will be indicated explicitly in the presentation of our numerical results.

For the zero-magnetic-field case, oscillations of the cluster as a whole with the characteristic frequency $\omega = \sqrt{2} \approx 1.414$ (i.e. the centre-of-mass oscillations; see reference [2]) do not couple with any other mode, and therefore will be taken out. For example, when we calculate the velocity autocorrelation function we give the velocity coordinates $\boldsymbol{v}_i$ with reference to the centre-of-mass velocity

$$\boldsymbol{v}_m = \frac{1}{N}\sum_i \boldsymbol{v}_i$$

and use the notation $\Delta\boldsymbol{v}_i(t) = \boldsymbol{v}_i(t) - \boldsymbol{v}_m(t)$. We calculated the velocity autocorrelation function

$$\tilde{Z}_t(\tau) = \left\langle \sum_i \Delta\boldsymbol{v}_i(t)\cdot\Delta\boldsymbol{v}_i(t+\tau)\right\rangle \Big/ \left\langle \sum_i \Delta\boldsymbol{v}_i(t)^2\right\rangle \tag{3}$$

and its components for radial motion

$$\tilde{Z}_r(\tau) = \left\langle \sum_i \Delta v_{i,r}(t)\Delta v_{i,r}(t+\tau)\right\rangle \Big/ \left\langle \sum_i \Delta v_{i,r}(t)^2\right\rangle \qquad v_{i,r} = (\boldsymbol{v}_i\cdot\boldsymbol{r}_i)/|\boldsymbol{r}_i| \tag{4}$$

and axial motion

$$\tilde{Z}_{\varphi}(\tau) = \left\langle \sum_i \Delta v_{i,\varphi}(t)\Delta v_{i,\varphi}(t+\tau) \right\rangle \Big/ \left\langle \sum_i \Delta \boldsymbol{v}_{i,\varphi}^2 \right\rangle \qquad v_{i,\varphi} = |\boldsymbol{v}_i \times \boldsymbol{r}_i|/|\boldsymbol{r}_i|. \tag{5}$$

The parentheses $\langle \cdots \rangle$ denote the averaging over time t. The spectrum of the velocity autocorrelation function is then defined as the Fourier transform

$$Z_{\alpha}(\omega) = 2\int_0^{\infty} \cos(\omega\tau)\tilde{Z}_{\alpha}(\tau)\ \mathrm{d}\tau. \tag{6}$$

3. Intershell rotation

In reference [2] an approximate Hamiltonian was obtained which was able to describe the intershell rotations:

$$H(\dot{\varphi}, \varphi) = \frac{1}{2}R_{\star}^2\dot{\varphi}^2 + \frac{1}{2}U_{\star}\left(1 - \cos\left(\frac{2\pi\varphi}{\varphi_{\star}}\right)\right) \tag{7}$$

where $U_{\star}$ is the barrier height, and $R_{\star}$, $\varphi_{\star}$ are defined below. The variable φ measures the angle of rotation of the shell with maximum angular velocity. For clusters with two shells,

$$R_{\star} = \sqrt{N_1 R_1^2 \gamma} \qquad \varphi_{\star} = \theta/\gamma \qquad \gamma = \left(1 + \frac{N_1 R_1^2}{N_2 R_2^2}\right)$$

where R_1, R_2 are the radii of the shells considered, N_1, N_2 are the number of particles within each shell, and $\theta = 2\pi/I$, where I is an integer, which is the minimal divisor of the numbers N_1, N_2. In the case in which the number of shells is $\geqslant 3$, the values for the parameters $R_{\star}$, $\varphi_{\star}$ are given in table 1 of reference [2]. Solving Hamiltonian (7) allows us to obtain the energy dependence of the angular velocity for intershell rotation:

$$V_{\varphi} = \left[\int_0^{2\pi} \frac{\mathrm{d}\varphi}{2\pi\dot{\varphi}}\right]^{-1} = \frac{\pi\sqrt{E/2}}{R_{\star}K(\sqrt{U_{\star}/E})} \tag{8}$$

where $K(x) \approx \pi/(1 + \sqrt{1 - x^2})$ is the complete elliptic integral. To analyse the region of applicability of these expressions and to check the validity of the method used to obtain the intershell rotation barriers $U_{\star}$, we also simulated the particle motion by the method of molecular dynamics. The initial conditions in this case were found to be as follows:

$$\boldsymbol{r}_i(t=0) = \boldsymbol{r}_{i,g}$$

$$\boldsymbol{v}_i(t=0) = \sqrt{2E}\,\boldsymbol{A}_{i,2} + \sum_{j=3}^{2N} \eta_j \boldsymbol{A}_{i,j}$$

where $\boldsymbol{r}_{i,g}$ are the coordinates of the particles in the ground state, and $\boldsymbol{A}_{i,j}$ are the eigenvectors of the dynamical matrix

$$H_{\alpha\beta,ij} = \frac{\partial^2 U}{\partial r_{\alpha,i}\,\partial r_{\beta,j}} \qquad \alpha, \beta = x, y \qquad i, j = 1, \ldots, N \tag{9}$$

which describe the different eigenmodes of the system. The eigenfrequencies and eigenvectors of this dynamical matrix were obtained in reference [2]. Here we consider the relation between the angular velocity and the kinetic energy E of the normal mode for intershell rotation. The coefficients η_j in the expression for the initial velocity were taken randomly from the Maxwellian distribution $f(\eta_j) = \sqrt{1/2\pi T}\exp(-\eta_j^2/2T)$.

The energy dependence of the angular velocity corresponding to the normal mode with the smallest eigenvalue is depicted in figure 1 for two different temperatures $T = 0$

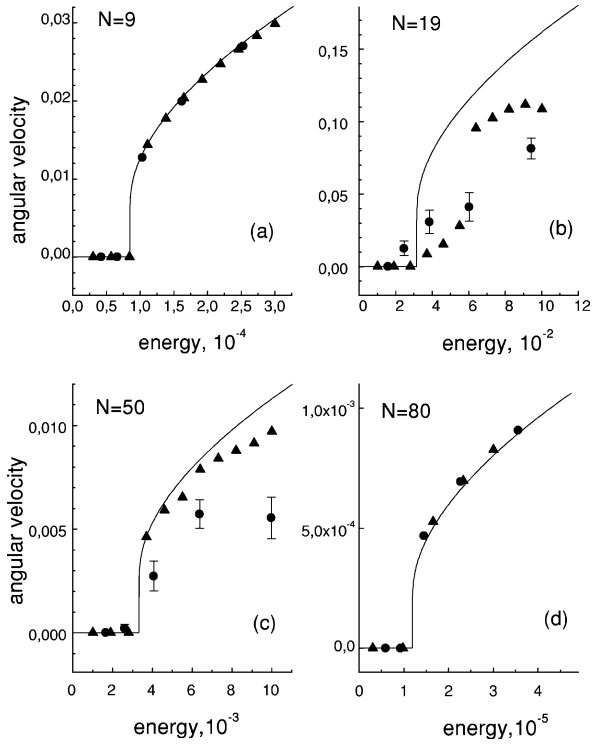

Figure 1. The angular velocity as a function of the energy of the cluster for different numbers of particles in the cluster: (a) $N = 9$, (b) $N = 19$, (c) $N = 50$ and (d) $N = 80$. The solid curve is derived from the analytical expression (8), and the triangles and circles are the results obtained by using the molecular dynamics method for $T = 0$ and $T = U_\star/2$, respectively. The angular velocity is in units of $\omega_0/\sqrt{2}$ and the energy in units of $(m\omega_0^2 q^4/2\epsilon^2)^{1/3}$.

(triangles) and $U_*/2$ (circles). As an example we took $N = 9$, 19, 50, 80 where the minimal eigenfrequencies $\omega_2 = \omega_{min}$ were given in reference [2] and are 0.1268, 0.667, 0.0754, 0.0184, respectively. The corresponding barrier heights for intershell rotation $U_\star$ are respectively 8.44×10^{-5}, 3.14×10^{-2}, 3.32×10^{-3}, 1.19×10^{-5}. We found that the intershell rotation barriers obtained earlier [2] agree with the ones calculated by the present method of molecular dynamics. Note that for clusters with small barrier height $U_\star$, i.e. for $N = 9$, 80, the simple model (7) which leads to the angular velocity (8) predicts the correct behaviour (full curves in figure 1). For configurations with a higher intershell rotation barrier height, the angular velocity is smaller than that given by the analytical expression (8). Such configurations correspond to ground states with high symmetry, in which the number of particles in the outer shell is a multiple of the number of particles in the inner shell. These are the so-called *magic number* clusters [2]. In this case we found that at non-zero temperature, rotation of the shell has already started at an energy which is less than the barrier height predicted by relation (8). This is attributed to *anharmonicity effects*, which become more important at higher energies. Note that the energy scales of figures 1(a), 1(d) and figures 1(b), 1(c) differ by at least an order of magnitude. As is apparent from figures 1(b), 1(c) for $E > U_\star$, the angular velocity is less than that predicted by relation (8). This effect can be ascribed to the importance of the radial distortion of the shell for angular rotations in the case of large energy, i.e. large temperatures.

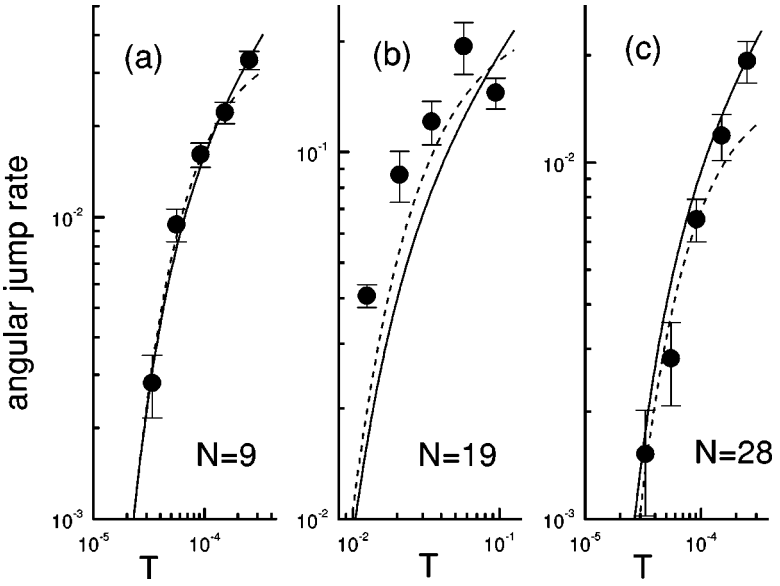

Figure 2. The intershell rotation rate or angular jump rate. The solid curves are the results derived from expression (10), and the dashed curves are obtained by using classical rate theory. The solid circles are the results from the present molecular dynamics study.

An alternative approach for analysing the behaviour of the cluster for non-zero temperatures is based on the average rotation frequency

$$R_a = \lim_{t\to\infty} \langle N_a(t)/t \rangle$$

for the shell with maximal angular velocity. In the above equation, N_a is the number of rotations over the angle $\varphi_\star$, and the averaging is carried out over the initial states of the cluster. Thus R_a is nothing but the angular jump rate for jumps over an angle $\varphi_\star$. Using our analytic model (7) we can calculate the angular jump rate by averaging the rotation velocity (8) over the Gibbs distribution with the Hamiltonian (7):

$$R_a = \left(\int \mathrm{d}\dot{\varphi}\ \mathrm{d}\varphi\ V_\varphi \exp\left(-H(\dot{\varphi},\varphi)/T\right)\right) \Big/ \left(\int \mathrm{d}\dot{\varphi}\ \mathrm{d}\varphi\ \exp\left(-H(\dot{\varphi},\varphi)/T\right)\right). \tag{10}$$

The integrals in equation (10) were performed numerically using an analytical approximation for the complete elliptic integral. From classical rate theory (see e.g. reference [10]) we have the following relation:

$$R_a = \frac{\omega_a}{\pi} \exp\left(-\frac{U_\star}{T}\right) \tag{11}$$

where

$$\omega_a = \prod_{i=2}^{2N} \omega_i \Big/ \prod_{i=3}^{2N} \omega_i^\star.$$

The eigenfrequencies ω_i refer to the eigenfrequencies of the normal modes of the ground state, while $\omega_i^\star$ corresponds to the eigenfrequencies of the state with maximum potential energy for intershell rotation. The latter is unstable and therefore $\omega_2^\star$ is imaginary, while the other $\omega_i^\star$ are real. The frequencies $\omega_i^\star$ were determined using the method of reference

[2]. We found that the value ω_a is slightly different from the eigenfrequency of the normal mode ω_2 which describes intershell rotation for a cluster in the ground state, e.g. for $N = 9$, 19, 28 the ratio is $\omega_2/\omega_a \approx 0.97$, 0.87, 1.07 respectively. In figure 2, a comparison is made between the expressions (10) (solid curves) and (11) (dashed curves) for the value of R_a as function of temperature. The numerical results (symbols in figure 2) are obtained by the method of molecular dynamics. Note that for clusters with low barrier heights (e.g. $U_\star \approx 8.44 \times 10^{-5}$, 8.31×10^{-5} for $N = 9$, 28 respectively) for intershell rotation, relation (10) agrees with the results of our molecular dynamics study within the statistical error. The results from classical rate theory (dashed curves in figure 2) underestimate the intershell rotation rate. For clusters with high energy barrier heights for intershell rotation (e.g. $N = 19$ in figure 2), expressions (10) and (11) lead to smaller values for R_a in the temperature range $T < U_\star$ ($\approx$0.031 for $N = 19$). This agrees with our previous study [2] which shows that for such cases the analysis of the behaviour of the harmonic normal modes gives a larger deviation from the pure numerical simulation, which is a consequence of the anharmonicity of the vibrations.

Table 1. The barrier heights for intershell diffusion obtained from the Monte Carlo simulations (U_m) for different numbers of particles (N).

N	5	6	9	10	12	14	15	16	17	18	19	20
U_m	0.149	0.134	0.064	0.047	0.057	0.065	0.141	0.084	0.067	0.134	0.064	0.145

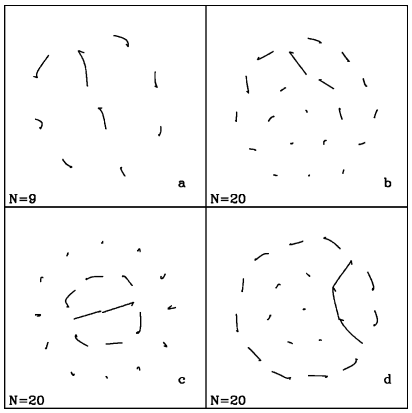

Figure 3. (a) and (b) depict trajectories corresponding to transitions from the ground state to a metastable state. (c) and (d) are examples of intershell diffusion without change of the numbers of particles in the shells.

4. Intershell diffusion

With increasing number of particles N in the cluster, an increasing number of metastable states are found with energy very close to the $T = 0$ ground-state energy. Between these metastable states and the actual ground state of the system there are potential barriers. At non-zero temperature the particles can borrow thermal energy in order to hop between these states. For N not too large, the lowest of these potential barriers is the barrier height for

intershell diffusion. For the cluster with six particles, the barrier height ($U_m \approx 0.135$) for transition from the ground state (1, 5) to the metastable state (6) was found in reference [11]. For this case the barrier was found by slowly moving the central particle to the periphery of the cluster. At each position of this particle the positions of all of the remaining particles were calculated by the Monte Carlo method from the condition of minimal energy. Here we follow a slightly different approach which is also suitable for treating large systems. Trajectories of the particles making a transition from the ground state to the metastable state were approximated by the polynomials

$$x_i = \sum_k \zeta_{x,ik} t^k,\ y_i = \sum_k \zeta_{y,ik} t^k \qquad t \in [0, 1]$$

where at $t = 0$ the system is in the ground state and at $t = 1$ we arrive in the metastable state. Varying t we calculate the maximum in the energy. This is the barrier height for some specific path in configuration space. Using the Monte Carlo technique and the Metropolis algorithm we vary the coefficients $\zeta_{x,ik}$, $\zeta_{y,ik}$ such that the minimal barrier height is obtained, which we identify as the barrier for intershell diffusion. Examples of such trajectories are plotted in figure 3 for different N. The calculated barrier heights for clusters with $N = 5, \ldots, 20$ are given in table 1. For the cluster of reference [11] consisting of six particles, we found the barrier height $U_m \approx 0.134$ which essentially coincides with the result of reference [11].

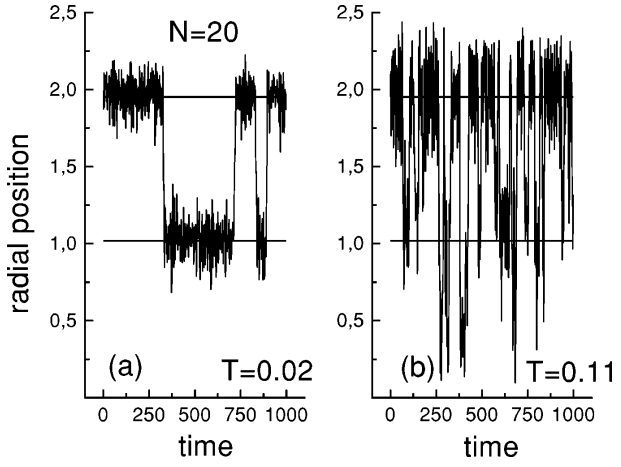

Figure 4. The time dependence of the radial position of a particular particle in a cluster with twenty particles for two different temperatures T. The two horizontal lines correspond to the radii of the different shells.

The above definition of the barrier height is based on the zero-temperature properties of the cluster. Now we consider an alternative approach in which we study the time dependence of the radial position ($\sqrt{x^2 + y^2}$) of the particles at some non-zero temperature. In figure 4 we show the radial position, as a function of time, of a certain particle for a cluster with $N = 20$ for two different temperatures. At low temperature the particle oscillates around its equilibrium position, which coincides with the characteristic radius of a certain shell of the cluster in its ground state. After some large time interval the particle can jump to its neighbouring shell. At large temperatures the overall picture of the motion remains the same but the frequency of jumps between the two shells is increased and the amplitude of the particle oscillation within one shell is much larger. We found that the total number

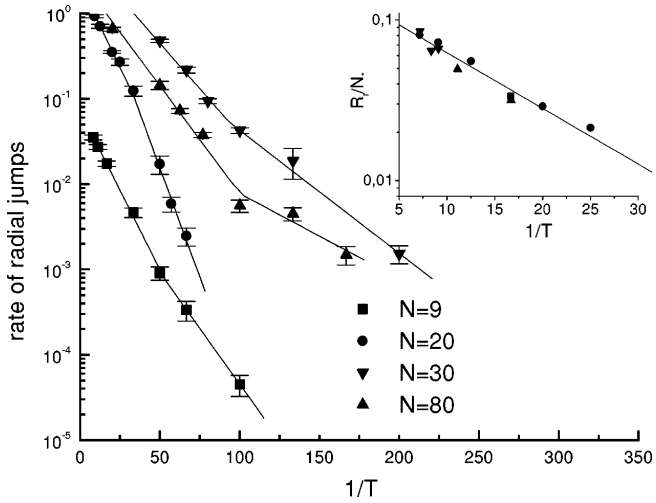

Figure 5. The radial jump rate for clusters with different numbers of particles. The solid lines are least-squares fits to an Arrhenius law and the symbols are the results of our molecular dynamics study. In the inset the reduced radial jump rate ($R_r/N_\star$) in the high-temperature region is shown for different numbers of particles in the cluster. The solid line is the fit to an Arrhenius law.

of radial jumps N_r of all of the particles in a cluster increases linearly with time. This is attributed to the diffusion nature of the particle motion. Therefore, we defined the rate of intershell jumps

$$R_r = \lim_{t\to\infty}\left\langle \frac{N_r(t)}{t} \right\rangle$$

where the averaging is carried out over the initial states of the cluster. This quantity is shown in figure 5 as a function of the inverse temperature. These numerical results can be well approximated by the Arrhenius law

$$R_r = A_r \mathrm{e}^{-U_r/T} \tag{12}$$

where the parameter A_r and the barrier height U_r may be different in regions of low ($T < T_r$) and high ($T > T_r$) temperatures. For clusters with $N = 9$, 20, 30, 80 the critical temperatures T_r are respectively 0.0188, 0.0299, 0.0100, 0.0107 which are comparable in magnitude to the melting temperatures found in [2]. In the low-temperature region we compare the results of this new definition with those from the above Monte Carlo analysis. For the cluster with $N = 9$ we found $U_r \approx 0.060$ which agrees approximately with our earlier determination (see table 1). But for the cluster with $N = 20$, the barrier height for intershell diffusion ($U_r \approx 0.118$) is less than the height of the lowest barrier between the metastable and the ground state $U_m = 0.145$. The same conclusion holds for clusters with $N = 30$, 80 where the barrier heights for intershell diffusion are respectively $U_r = 0.023$ and $U_r = 0.033$. This tells us that for large clusters, intershell diffusion is determined by the simultaneous transition of two particles between two shells without a change in the occupancy of the shells, while for small clusters intershell diffusion can rather be described as transitions between the ground state and metastable states. Because this mechanism is responsible for the melting of the ring structure of the classical cluster, the microscopic classical melting behaviours for small N and large N are different.

Figures 3(a), 3(b) show the transitions of the clusters with $N = 9$ (a) and $N = 20$ (b) from the ground states (2, 7), (1, 7, 12) to the metastable states (1, 8), (1, 6, 13) respectively. Figures 3(c), 3(d) show the simultaneous transition of two particles from one shell to a neighbouring one for a cluster with $N = 20$ without a change of the occupancy of each of the shells. Because the particles are identical, the state is not altered after such a transition. We have tried to obtain the barrier height using the Monte Carlo technique described above by taking initial and final states of the cluster corresponding to transitions which do not change the number of particles on the different shells. This led for the case of figures 3(c), 3(d) to the barrier heights 0.210 and 0.149. Notice that also in this case for the cluster with $N = 20$ particles the barrier heights are higher than the ones found by the method of molecular dynamics which indicates an appreciable softening of the barrier due to temperature effects. We think that the mechanism behind this is the energy exchange between different modes which plays an essential role in the transition process, and consequently the particle trajectories have a more complicated form than found using the above Monte Carlo simulation. Figure 3(d) indicates vortex-like motion, which corresponds to the rotation of a pentagon which is located at the periphery. As found from our computer simulations, the barrier heights corresponding to rotations of polygons are rather insensitive to the numbers of particles which are involved. Consequently, the number of possible collective motions of the particles which involve intershell diffusion increases very fast with the number of particles in the cluster. This is why for large clusters the definition of a simple energy barrier and the use of classical rate theory are no longer appropriate because of the presence of an almost continuous spectrum of excitations for intershell diffusion.

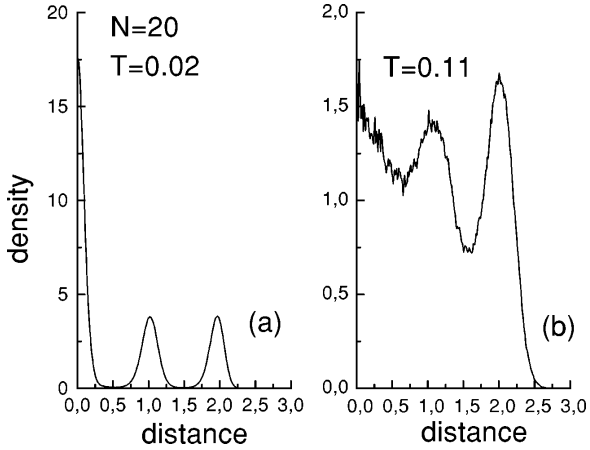

Figure 6. The radial distribution of the particle density for a cluster with 20 particles at two different temperatures.

For low temperatures, the barrier to intershell diffusion is determined by the number of particles within the cluster. If the temperature exceeds some critical value T_r, the barrier heights for the different clusters become approximately equal. The value of the critical temperature T_r is smaller than the cluster melting temperature which was obtained previously using the Lindemann criterion [2]. The factor A_r in expression (12) rises as the number of particles increases. Let us assume that for $T > T_r$ the energy barrier height for diffusion is the same for all shells within the cluster. Then the rate of intershell diffusion is proportional to the effective number of particles $N_\star = N - N_{out}/2$, where N_{out} is the number of particles in the most outer shell, where jumps can only be in one direction. As one can see from the

inset of figure 5, in the high-temperature range the rate of radial jumps per particle, $R_r/N_\star$, depends only very weakly on the total number of particles. The resulting energy barrier height for $T > T_r$ is approximately equal to 8.9×10^{-2} and practically *independent* of the number of particles. Thus in the low-temperature range the energy barrier height for radial jumps attains a universal value.

Vanishing of the large maxima in the radial particle density is a signature of the transition from the crystalline-like state to the liquid-like state (see figure 6). Note that even in the liquid state some shell-like structure still remains although there is already a large probability of finding the particle between the shells. Thus the liquid state is not homogeneous but its density is radially modulated. It is interesting that during the phase transition for radial melting the barrier height for intershell diffusion increases or decreases, depending on the number of particles in the cluster (see figure 5). For large clusters and at low temperature the transition occurs generally between the outer shells, for which the energy barrier for the rotation of a part of the cluster is smaller. Therefore the prefactor A_r in equation (12) grows in this case when the cluster melts and all particles start to take part in the diffusion process.

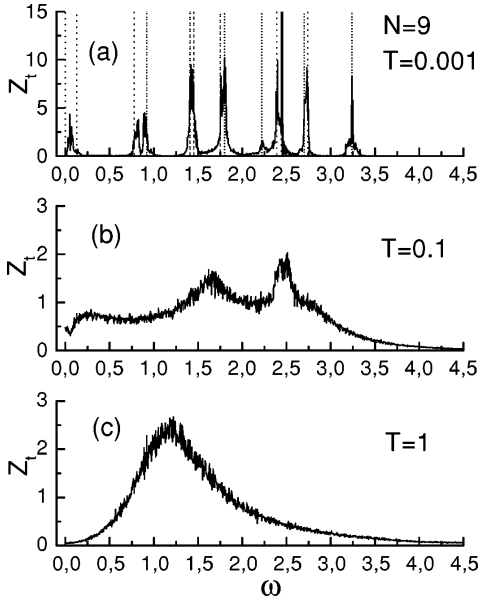

Figure 7. The frequency spectrum of the velocity autocorrelation function for a cluster with nine particles for different temperatures. The dotted lines correspond to the eigenfrequencies at zero temperature. The frequency is in units of $\omega_0/\sqrt{2}$.

5. The velocity autocorrelation function

In the two previous sections we studied the angular and radial jump rates for particle motion in a classical atom. Now we will follow the complete time-dependent motion of the different particles. We therefore calculate the spectrum of the velocity autocorrelation function (3) and investigate whether we can find any signature of melting. For zero temperature such spectra consist of a series of delta functions which are located at the frequencies of the excitation spectrum, which were calculated in reference [2]. With increasing temperature

these delta functions broaden and at sufficiently high temperature a continuous spectrum is found (see figure 7 for $N = 9$). The dotted vertical lines in figure 7(a) correspond to the zero-temperature case. Notice that for low temperature (see figure 7(a)) the effect of temperature is twofold: it broadens the zero-temperature delta functions in the velocity autocorrelation function and it couples those frequencies which differ very little with each other in energy.

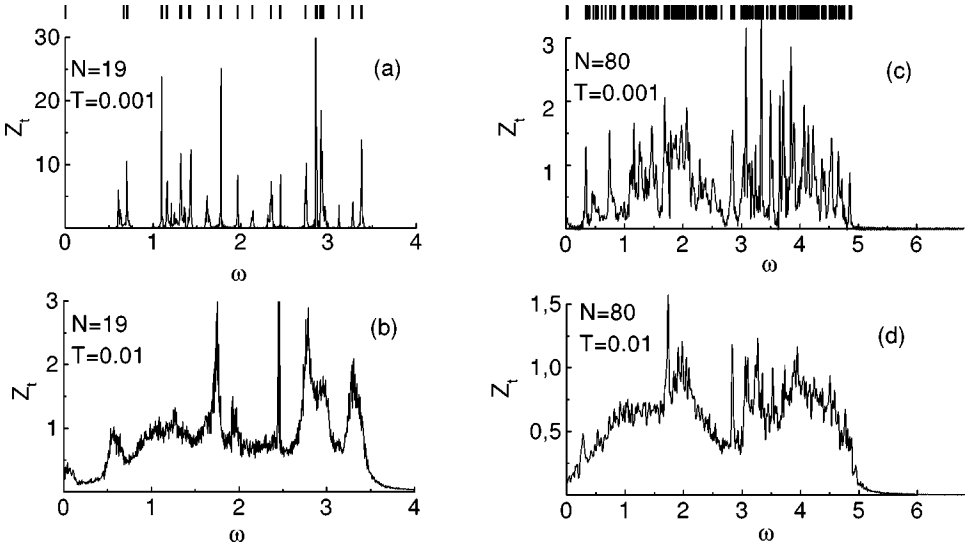

Figure 8. The spectra of the velocity autocorrelation functions for clusters with two different numbers of particles and for two different temperatures. The position of the $T = 0$ eigenfrequencies are indicated by the vertical lines at the tops of the figures.

For clusters with a small barrier height for intershell rotation, anharmonicity is only essential for the normal mode with the lowest eigenfrequency ω_2, which is the frequency for angular vibrations. Therefore, in the temperature range $U_\star \ll T \ll T_\star$, where $T_\star$ is the temperature for cluster melting, there is a region in the spectrum $0 < \omega < \omega_2$ (see the low-frequency behaviour in figure 7(a)) where the peak corresponds to relative rotations of the shells. In figure 8 similar plots are made for larger clusters. The positions of the $T = 0$ eigenfrequencies are indicated by the vertical bars at the tops of the figures. There is no sudden change in the spectrum when we cross the melting region which is similar to what was observed for 3D clusters [5]. Notice also that there are a number of peaks which stay rather sharp even at relatively large temperature. The reason for this is that the excitations with such frequencies couple only very weakly to the other frequencies. An example of such a frequency is the breathing mode in figure 8(a) which has $\omega = \sqrt{6} \approx 2.45$ at zero temperature. In appendix A we derive analytically the eigenfrequency of this mode, for an arbitrary number of particles in the cluster, from which it is apparent that there is almost no coupling with the other harmonic modes of the cluster.

Fluctuations in the particle motion cause the overlap between neighbouring levels and result in the formation of a continuous spectrum in the autocorrelation function. At low temperatures this becomes first apparent in the frequency range between eigenmodes which are close in frequency (see figure 7(a)). With increasing number of particles, the difference in eigenfrequencies reduces and chaotization of the motion occurs at lower temperature. This phenomenon is already apparent before melting occurs in the case of large clusters

(see figure 8 for $N = 80$ and $T = 0.001$). For large clusters the existence of two broad maxima in the excitation spectrum is related to the excitation of acoustic and plasma-type waves with different characteristic frequencies (see e.g. reference [2]). This is analogous to an infinite Wigner crystal [12–14] where such acoustic and optical modes are present in the phonon spectrum. The density of the phonon states of the Wigner crystal at zero frequency is proportional to the self-diffusion coefficient [7] which in a finite system has to be exactly equal to zero. Therefore, at large temperatures and with increasing frequency the value $Z(\omega)$ abruptly increases from zero at $\omega = 0$ to some finite value for $\omega \neq 0$ which further weakly depends on frequency (see e.g. figure 7(b) for $N = 9$ and $T = 0.1$).

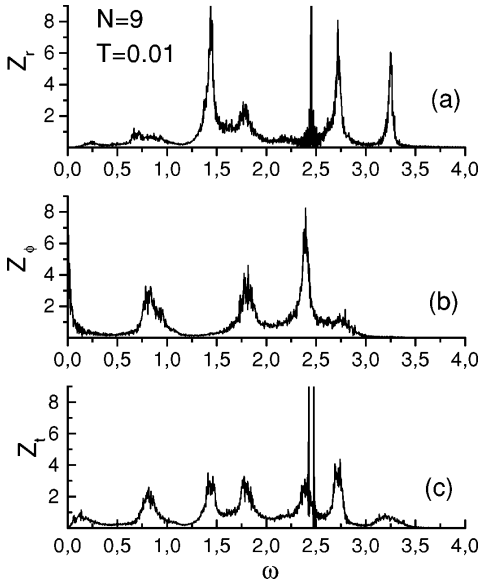

Figure 9. The spectra of the (a) radial, (b) angular, and (c) total velocity autocorrelation functions for a cluster with nine particles for a fixed temperature $T = 0.01$.

Because of the circular symmetry of our system we expect a large difference between the angular and the radial response (see figure 9). This is also expected from the fact that angular melting occurs at a lower temperature than radial melting. For sufficiently large cluster sizes, we found that this distinction disappears, which agrees with our previous observation [1] that for such a system the angular and radial melting temperatures coincide. Notice that Z_t is not simply the sum of Z_φ and Z_r because cross-terms are present. Furthermore, $Z_r(0) = 0$ while $Z_\varphi(0) \neq 0$ due to intershell rotation. In figure 9(c) we find two very sharp peaks in Z_t at $\omega_1^* \approx 2.427$ and $\omega_2^* \approx 2.477$ which are a result of the splitting of the breathing mode in Z_r which occurs at $\omega = \sqrt{6} = 2.449$. This splitting occurs because of the mixing with intershell rotation (i.e. the lowest non-zero frequency $\omega_2 = 0.067$) which occurs with the small frequency $\Delta\omega = \omega_2^* - \omega_1^* \approx 0.050$.

6. The influence of a magnetic field

It is known [15] that in a classical system an external magnetic field does not alter the statistical properties of the system, and consequently the melting temperatures will be insensitive to the magnetic field strength. But on the other hand, the character of the

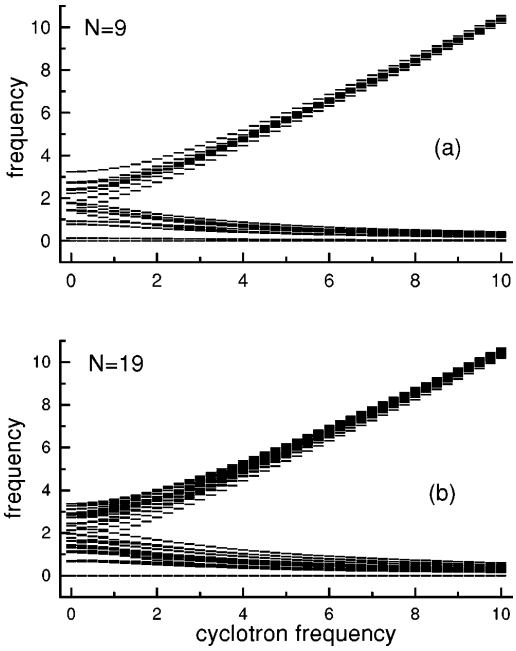

Figure 10. The excitation spectra of two clusters with different N as functions of external magnetic field.

motion of the particles is altered significantly when the cyclotron frequency is larger than the eigenfrequencies of the system. The spectrum of an infinite 2D Wigner crystal in a magnetic field was obtained in [12, 13]. Here we will be interested in finite systems. For the definition of the spectrum of a finite system in a magnetic field, we Fourier transform the Newton equations

$$\tilde{H}_{\alpha\beta,ij}Q_{\beta,j} = (\omega^2\delta_{\alpha\beta,ij} - H_{\alpha\beta,ij} + \mathrm{i}\omega\omega_c E_{\alpha\beta}\delta_{ij})Q_{\beta,j} = 0$$

where $E_{\alpha\beta z}$ is the Levi–Civita tensor, δ_{ij} and $\delta_{\alpha\beta,ij}$ are unit matrices, and $Q_{\beta,j}$ is the particle displacement from its equilibrium position. To determine the spectrum we calculate the roots of the determinant of the Hermitian matrix $\tilde{H}_{\alpha\beta,ij}$. The determinant was calculated after reducing the matrix to a triangular form using Gaussian elimination. The general qualitative behaviours of the magnetic field dependence of the excitation spectrum are very similar for clusters with different numbers of particles (figure 10). As in an infinite system [12], there are two branches in the spectrum which contain the same number of eigenfrequencies. The high-frequency branch describes the orbital particle motion with frequency near the cyclotron frequency. The low-frequency branch corresponds to particle drift with a frequency which is inversely proportional to the magnitude of the magnetic field. For completeness we mention that for a classical dot in the liquid state the magnetoplasma excitations in harmonic and anharmonic electron dots were considered in references [16, 17].

Typical trajectories of the particles in a dot with $N = 9$ at a temperature $T = 0.06$ are shown in figure 11. The influence of the magnetic field is clearly apparent when we compare figure 11(a) with figure 11(b). With increasing magnetic field the difference between the eigenfrequencies of each of the branches of the spectrum decreases considerably. Therefore, already at low temperature the spectrum of the velocity autocorrelation function has become continuous for each branch (figure 12). At the same time there is some small

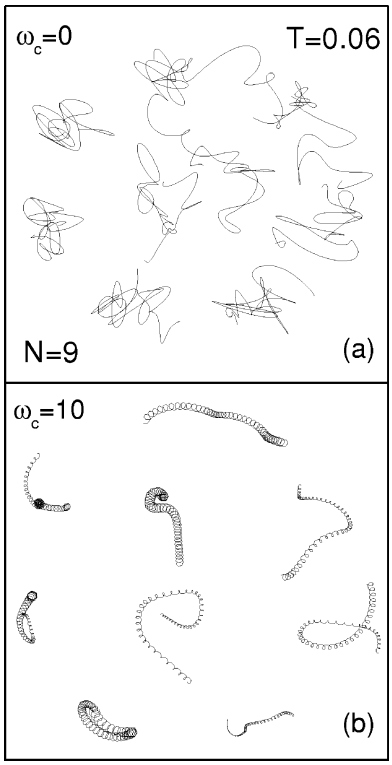

Figure 11. The trajectories of particles at a temperature $T = 0.06$ in the presence and the absence of an external magnetic field for $N = 9$.

energy exchange between the two branches which is due to anharmonicity effects.

In a strong magnetic field the main part of the kinetic energy belongs to the orbital particle motion. Therefore in expressions (11) and (12) which describe the rate of intershell rotation and intershell diffusion, the prefactors (ω_a/π, A_r) have to be reduced while the energy barrier height does not depend on the magnetic field strength. The drift velocity of the centre of the orbit is determined by the expression

$$\boldsymbol{v}_{d,i} = -\boldsymbol{\omega}_c \times \boldsymbol{F}_i/\omega_c^2$$

where $\boldsymbol{F}_i = -\partial U/\partial \boldsymbol{r}_i$ is the force acting on particle i. In the harmonic approximation we have

$$\boldsymbol{F}_i = -\sum_{j=1}^{2N} \omega_j^2 q_j \boldsymbol{A}_{i,j}$$

where the $\boldsymbol{A}_{i,j}$ are the eigenvectors of the dynamical matrix (9). Using the Gibbs distribution for the amplitude of the normal modes q_j:

$$f(q_j) = \sqrt{\frac{\omega_j}{2\pi T}} \exp\left(-\frac{\omega_j^2 q_j^2}{2T}\right) \tag{13}$$

we obtain the expression for the mean energy of the drift of the particles:

$$U_d = \frac{1}{N}\sum_{i=1}^{N} \frac{v_{d,i}^2}{2} = \frac{T}{N\omega_c^2}\sum_{i=1}^{2N} \omega_i^2.$$

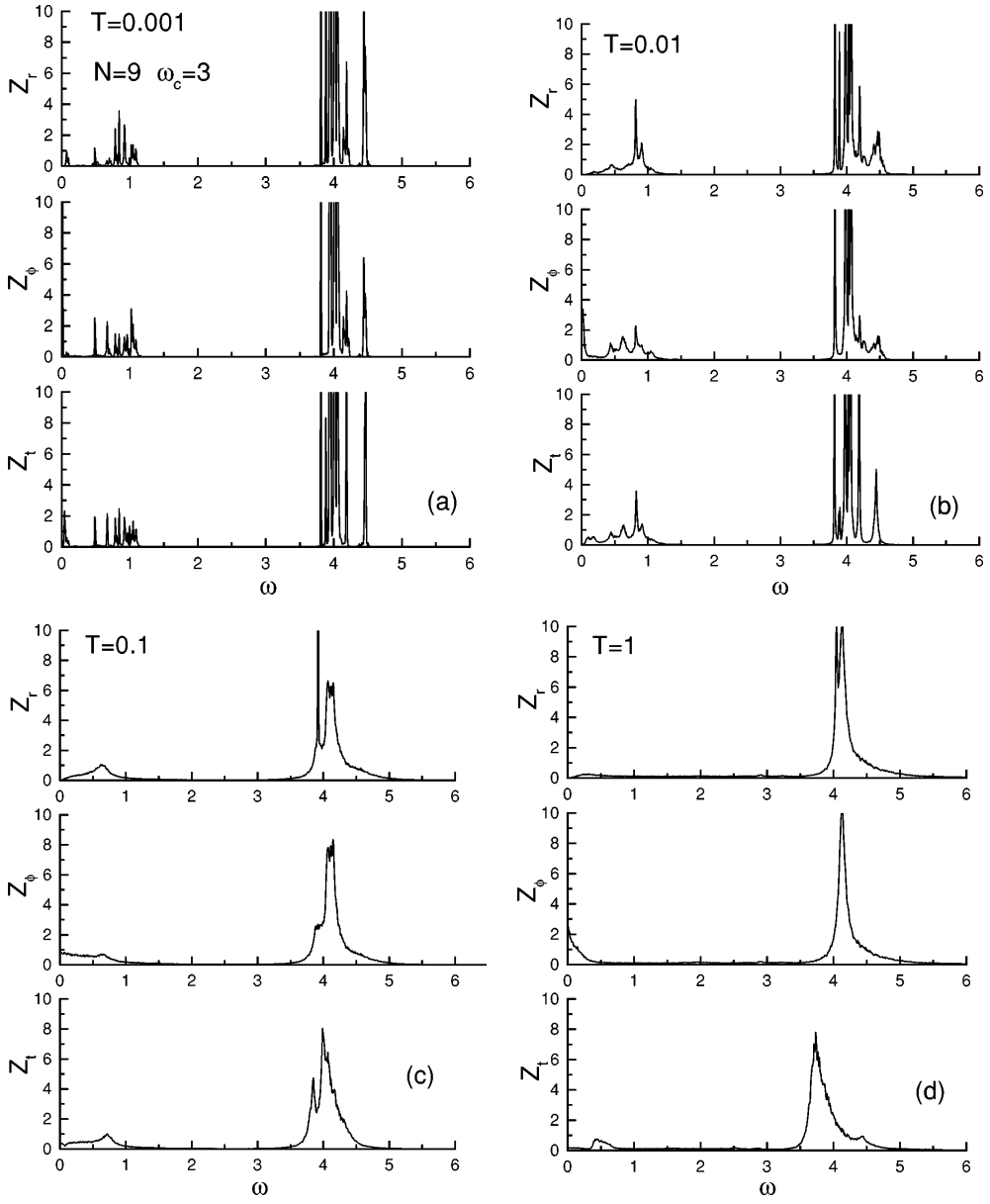

Figure 12. The spectrum of the velocity radial (Z_r), angular (Z_ϕ), and total (Z_t) autocorrelation functions for a cluster with nine particles in the presence of a fixed magnetic field and for four different temperatures: (a) $T = 0.001$, (b) $T = 0.01$, (c) $T = 0.1$, and (d) $T = 1$.

We also investigated the influence of a magnetic field on the intershell rotation rate and the intershell diffusion rate within the framework of classical rate theory. It is necessary to determine first the absolute value of the drift velocity at the point $\boldsymbol{r}_{i,m}$ for the state with maximum potential energy. Methods of defining this point for intershell diffusion were described above. Diagonalizing the dynamical matrix (9) by the Householder method we obtain eigenvalues and eigenvectors at the point $\boldsymbol{r}_{i,m}$. The eigenvector $\boldsymbol{A}_{i,1}$ having

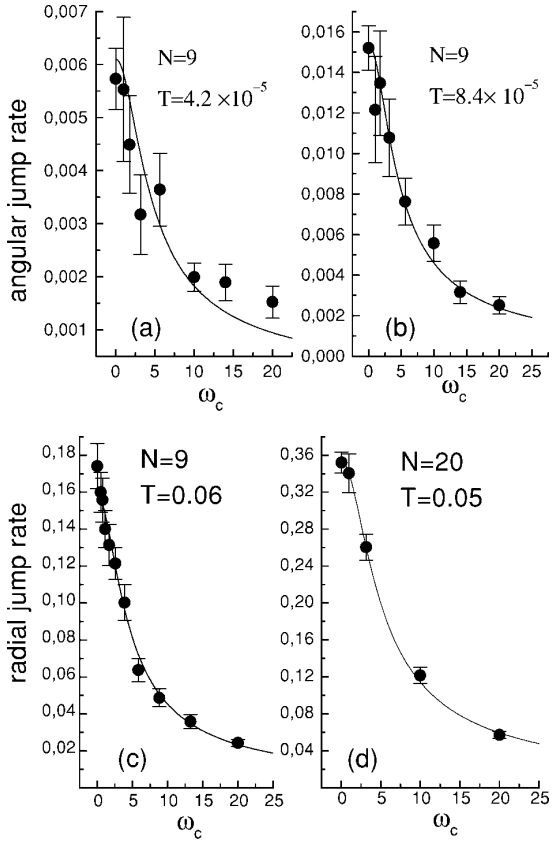

Figure 13. The angular, (a), (b), and radial, (c), (d), jump rates for a cluster with nine, (a), (b), (c), and twenty, (d), particles and for different temperatures. The solid curves are the results obtained by using expression (14), and the points are the results from our molecular dynamics study.

an imaginary eigenvalue describes the transition from one equilibrium state to another through the maximum of the potential barrier. All of the remaining eigenvalues are real. The eigenvectors corresponding to $\boldsymbol{A}_{i,k>1}$ are orthogonal to those corresponding to $\boldsymbol{A}_{i,1}$ and describe the vibration of the particles in the vicinity of the energy maximum. The projection of the drift velocity onto the vector $\boldsymbol{A}_{i,1}$ is given by

$$V_d = -\omega_c^{-1} \sum_{\alpha=1}^{2} \sum_{\beta=1}^{2} \sum_{i=1}^{N} \sum_{k=2}^{2N} A_{\alpha,i1} E_{\alpha\beta z} \omega_k^2 q_k A_{\beta,ik}.$$

To determine the mean value of $|V_d|$, integrals over normal coordinates which are distributed according to the probability distribution (13) were used in a Monte Carlo simulation. The ratio $V_d/V_t = \omega_\star/\omega_c$ which is the drift velocity over the thermal velocity $V_t = \sqrt{T/2\pi}$ does not depend on temperature and is inversely proportional to the magnetic field. The excitation spectrum of the normal modes of the transition state corresponds to the potential energy maxima, which do not differ significantly with the ground-state spectrum. Therefore, the parameters $\omega_\star$ for intershell rotation ($N = 9$, $\omega_\star \approx 1.25$) and intershell diffusion ($N = 9$, $\omega_\star \approx 1.19$) are approximately equal. Since the amplitudes of normal modes are inversely proportional to their frequencies, the characteristic frequency $\omega_\star$ corresponds to

the arithmetic mean value of the frequencies of the normal modes. For a weak magnetic field it is not difficult to show that the change of velocity of the particles is proportional to the square of the cyclotron frequency. Therefore to analyse the influence of a magnetic field on the intershell diffusion rate and the intershell rotation rate we used the approximate formula

$$R_H = R(H=0)\frac{\omega_\star}{\sqrt{\omega_\star^2+\omega_c^2}} \tag{14}$$

where $R(H=0)$ is calculated in zero magnetic field. Expression (14) is compared in figure 13 with the results of our molecular dynamics study. Note that in ionized gases the diffusion coefficient in a strong magnetic field changes inversely proportionally to the cyclotron frequency because diffusion is determined by jumps from one cyclotron orbit to another one. In the case of a continuous medium, a particle is in the field of its neighbouring particles, and the decrease of the diffusion coefficient is connected to the reduction of the characteristic value of the drift velocity.

7. Conclusion

We have presented the results of a molecular dynamics study of the motion of charged classical particles in a finite 2D system, confined by a parabolic potential. The intershell rotation rate and intershell diffusion rate were obtained. The temperature dependence of the diffusion rate is described by an Arrhenius law. In the low-temperature region, when the system is in the crystalline state, the energy barrier height depends on the number of particles in the cluster. For large clusters, diffusion is determined by the simultaneous transition of two particles from one shell to a neighbouring one without any change in the local density. At the periphery of the cluster, rotations of polygons of particles are possible. This process has a small potential barrier height and therefore is favoured. In the liquid-like state, probabilities for intershell jumps are practically independent of the effective number of particles in the cluster. When the cluster melts, the energy barrier height can either increase or decrease, depending crucially on the number of particles in the cluster. We also found that the velocity autocorrelation function does not exhibit any clear signature of the melting transition. An external magnetic field changes only the prefactor in the relation between the rate of jumps and temperature. In a strong magnetic field, the rates of intershell rotation and intershell diffusion change inversely proportionally to the cyclotron frequency.

Acknowledgments

We wish to thank our colleague V M Bedanov for fruitful discussions. Part of this work was supported by INTAS-93-1495-ext, the Human Capital and Mobility network Programme No ERBCHRXT 930374, the Flemish Science Foundation (FWO), and the Russian Foundation for Basic Research 96-02-19134. One of us (FMP) is a research director with the FWO.

Appendix A

Here we will derive the eigenfrequency corresponding to the breathing mode in the case in which an arbitrary external magnetic field is applied perpendicularly to the system. Let $\boldsymbol{M} = \sum_i \boldsymbol{r}_i \times \boldsymbol{v}_i$ be the total angular momentum, where $\boldsymbol{v}_i = \partial \boldsymbol{r}_i/\partial t$ is the velocity of

particle i. Notice that for our system (1) the vector

$$\boldsymbol{M} + \frac{1}{2}\boldsymbol{\omega}_c \sum_i r_i^2 = \boldsymbol{M}_0 \tag{A1}$$

is an integral of motion. Using total energy conservation $E = U + T$, where U is the potential energy, and $T = \sum_i \boldsymbol{v}_i^2/2$ is the kinetic energy, the equation for the mean square radius $R = \sum_i r_i^2/N$ can be written as

$$\frac{\partial^2 R}{\partial t^2} = -6R + 2(\boldsymbol{\omega}_c \cdot \boldsymbol{M} + E + T)/N. \tag{A2}$$

Using condition (A1) one can reduce the above equation to

$$\frac{\partial^2 R}{\partial t^2} = -(6 + \omega_c^2)R + 2(\boldsymbol{\omega}_c \cdot \boldsymbol{M}_0 + E + T)/N. \tag{A3}$$

The above equation tells us that the eigenfrequency of the breathing mode is $\omega = \sqrt{6 + \omega_c^2}$. At zero temperature, $\boldsymbol{v}_i = 0$, and consequently $T = 0$ and $\boldsymbol{M} = 0$ which implies that the mean square radius becomes $R = E/3N$ and $\boldsymbol{M}_0 = \boldsymbol{\omega}_c E/6$. Since the fluctuations of the total kinetic energy are small at finite temperature, there will be only a weak coupling between the breathing mode and the other modes of the system.

The frequency of the above breathing mode was found first in reference [2]. Recently, similar breathing modes were found in the quantum dot system in which case the frequency may be different [18].

References

[1] Bedanov V M and Peeters F M 1994 *Phys. Rev.* B **49** 2667
[2] Schweigert V A and Peeters F M 1995 *Phys. Rev.* B **51** 7700
[3] Peeters F M, Schweigert V A and Bedanov V M 1995 *Physica* B **212** 237
Schweigert V A and Peeters F M 1994 *Superlatt. Microstruct.* **16** 243
[4] Lozovik Yu E and Pomirchy L M 1990 *Phys. Status Solidi* b **161** K11
[5] Lozovik Yu E and Mandelshtam V A 1990 *Phys. Lett.* **145A** 269
Lozovik Yu E and Mandelshtam V A 1992 *Phys. Lett.* **165A** 469
[6] Hansen J-P, Levesque D and Weis J J 1979 *Phys. Rev. Lett.* **43** 979
[7] Hansen J-P and McDonald I R 1980 *Theory of Simple Liquids* (New York: Academic)
[8] Landau L D and Lifshitz E M 1980 *The Classical Theory of Fields* (Oxford: Pergamon)
[9] Metropolis N, Rosenbluth A W, Rosenbluth M N, Teller A M and Teller E 1953 *J. Chem. Phys.* **21** 1087
[10] Robinson P L and Holbrook K A 1972 *Unimolecular Reactions* (New York: Wiley–Interscience)
[11] Bolton F and Rössler U 1993 *Superlatt. Microstruct.* **13** 139
[12] Chaplik A V 1972 *Sov. Phys.–JETP* **35** 395
[13] Bonsall L and Maradudin A A 1977 *Phys. Rev.* B **15** 1959
[14] Bedanov V M, Gadiyak G V and Lozovik Yu E 1985 *Phys. Lett.* **108A** 448
[15] Van Leeuwen J H 1921 *J. Physique* **6** 361
Kubo R 1965 *Statistical Mechanics* (Amsterdam: North-Holland) (see problem 27 of chapter II)
[16] Shikin V, Nazin S, Heitmann D and Demel T 1991 *Phys. Rev.* B **43** 11 903
[17] Ye Z L and Zaremba E 1994 *Phys. Rev.* B **50** 17 217
[18] Maksym P 1995 *Europhys. Lett.* **31** 405
Johnson N F and Quiroga L 1995 *Phys. Rev. Lett.* **74** 4277
Geller M R and Vignale G 1996 *Phys. Rev.* B **53** 6979